EXPRESS

Open Access

CrossMark

LSMO Nanoparticles Coated by Hyaluronic Acid for Magnetic Hyperthermia

Yuanwei Chen[1], Ying Wang[1*], Xi Liu[2], Mai Lu[2], Jiangwei Cao[1] and Tao Wang[1*]

Abstract

Magnetic hyperthermia with the treating temperature range of 41–46 °C is an alternative therapy for cancer treatment. In this article, lanthanum strontium manganates ($La_{1−x}Sr_xMnO_3$, $0.25 \leq \times \leq 0.35$) magnetic nanoparticles coated by hyaluronic acid (HA) which possesses the ability of targeting tumor cells were prepared by a simple hydrothermal method combined with a high-energy ball milling technique. The crystal structure, morphology, magnetic properties of the HA-coated magnetic nanoparticles (MNPs), and their heating ability under alternating magnetic field were investigated. It was found the HA-coated $La_{0.7}Sr_{0.3}MnO_3$, with particle diameter of ~100 nm, Curie temperature of 45 °C at a concentration 6 mg/ml, gave the optimal induction heating results. The heating temperature saturates at 45.7 °C, and the ESAR is 5.7×10^{-3} W/g · kHz · (kA/m^2) which is much higher than other reported results.

Keywords: LSMO, Functionalization, Magnetic hyperthermia, Hyaluronic acid

Background

Magnetic hyperthermia is considered as an alternative therapy for cancer treatment since it has no side effect compared with traditional drugs or radiation treatment [1, 2]. Magnetic nanoparticles (MNPs) in stable colloidal suspensions can be delivered to tumor via non-invasively route and heated with external high-frequency magnetic field. The treating temperature of target tissue should be 41–46 °C to destroy the cancer cells while avoiding the harm on normal cells [3]. To prevent treating temperature to a higher value, a thermometry probe contacting with target tissue is always needed [4, 5]. However, this method is harmful when tumor is inside the body. If the heating of MNPs can stop automatically when temperature is up to 46 °C, the thermometry probe can be omitted. For the sake of achieving this purpose, the series of $La_{1−x}Sr_xMnO_3$ (LSMO) compounds has attracted great interest in recent years [6–8]. The ferromagnetic–paramagnetic transition temperature T_c (Curie temperature) of LSMO compounds is from 10 to 97 °C with the variation of Sr content [9]. Above the T_c, MNPs lose the ability of generating caloric under

magnetic field. By controlling the contents precisely, LSMO MNPs can reach a saturation heating temperature around 46 °C without adjusting external magnetic field.

The most popular method of preparing LSMO nanomaterial is sol-gel method, whereas the aggregation of nanograins is serious [10]. Another possible method is hydrothermal method, but the grain size and shape of the production are hard to control [11]. Both of these method need further smashing of the productions if monodisperse MNPs are desired. Meanwhile, a surfactant is necessary for prohibiting the agglomeration of MNPs in magnetic fluid and improving the biocompatibility [12].

In this work, LSMO MNPs was prepared by a simple hydrothermal method and then smashed by high-energy ball milling technique. Moreover, hyaluronic acid (HA) is a naturally occurring polysaccharide present in the extracellular matrix and synovial fluids. It can specifically bind to various cancer cells, and its conjugates containing anti-cancer agents exhibit enhanced targeting ability to the tumor and higher therapeutic efficacy compared to free anti-cancer agents. In this work, HA was used as the surfactant of the prepared LSMO MNPs. The basic physical properties and heating effect of the HA-covered MNPs under high frequency magnetic field were investigated.

* Correspondence: yingw@lzu.edu.cn; wtao@lzu.edu.cn
[1]Key Laboratory for Magnetism and Magnetic Materials of the Ministry of Education, Lanzhou University, Lanzhou 730000, China
Full list of author information is available at the end of the article

Chen *et al. Nanoscale Research Letters* (2016) 11:538

Page 2 of 6

Methods

La$_{1-x}$Sr$_x$MnO$_3$ (0.25 ≤ × ≤ 0.35) nanoparticles were synthesized by a simple hydrothermal method combined with high-energy ball milling technique [13, 14]. In the reactive hydrothermal method, La(NO$_3$)$_3$ · 6H$_2$O, Sr(NO$_3$)$_3$, KMnO$_4$, Mn(CH$_3$COO)$_2$ · 4H$_2$O, and KOH were added to 100-ml deionized H$_2$O in appropriate proportions. The total molar amount of La^{3+} and Sr^{2+} ions was 0.0125 mol. In order to keep the balance of charges, the amount of Mn^{2+} and Mn^{7+} ions differs with the doping of Sr^{2+} while the total molar amount of them was 0.0125 mol. KOH was used as a mineralizer, and its amount was 0.8 mol. The reaction mixture was then sealed in Teflon-lined stainless steel autoclaves and heated at 220 °C for 48 h. The production was decanted in magnetic field several times to remove additional ions. Before the ball milling, 0.3 g of surfactant and 1.0 g of LSMO powder were added. The pH of the mixture was adjusted to 5 by dilute hydrochloric acid. High-energy ball milling was carried out for 8 h to form the LSMO magnetic nanofluid [2, 12]. To reduce agglomeration of the magnetic particles, the milled nanoparticles were dispersed in NaOH solution with the pH = 12. HA-coated LSMO (x = 0.25, x = 0.3, x = 0.35) MNPs were denoted by S1, S2, and S3, respectively. As a contrast, OA (oleic acid)-coated La$_{0.7}$Sr$_{0.3}$MnO$_3$ MNPs was also fabricated and denoted by S4 [12].

The purity, homogeneity, and crystal structure of samples were characterized by X-ray diffractometer (Philips X'pert). The Scherrer equation was used to determine the size of the crystallites using the most intense peak in all cases, which appears at approximate 32.79°. The surface morphology of the samples was observed using scanning electron microscopy (SEM, Hitachi S-4800) (Additional file 1). The particle size was determined by high-resolution transmission electron microscopy (HRTEM, TecnaiTM G2F30, FEI). The hysteresis loops were measured using a vibrating sample magnetometer (The ADE Model EV9 system) at 300 K. Curie temperature was determined as the minimal value of dM/dT versus *T* curves. The thermal heating curves of magnetic liquids were obtained from SPG–I high-frequency induction heating equipment. The magnetic field of the coil was calculated by the relation:

$$H = \frac{1.257 \times N \times I}{L},$$

in which *N*, *I*, and *L* represent the number of turns, applied current and diameter of the turn in centimeter, respectively [15]. The used magnetic fields here are 53.1 Oe. The temperature variation was measured using an optical fiber probe.

The heating capacity of MNPs is quantified by the SAR (specific absorption rate) value according to the following relation [12, 16, 17]:

$$SAR = C_w \frac{\Delta T}{\Delta t} \frac{1}{m_{magn}},$$

where C_W is the specific heat capacity of water (4.18 J g^{-1}K^{-1}), $\Delta T/\Delta t$ is the initial slope of the time dependent temperature curve. The value of m_{magn} is the weight fraction of the magnetically active element. It should be noted that SAR strongly depends on magnitude and frequency of the applied magnetic field, so experiment results from disparate studies using disparate magnetic field are difficult to compare. In order to directly compare the SAR of our samples with the other reported values, the effective specific absorption rate (ESAR) was also calculated. The ESAR is a heating transformation ability which normalizes SAR with respect to field strength and frequency. It is expressed as follows: [8, 16, 18, 19]:

$$ESAR = \frac{SAR}{H_{applied}^2 f},$$

where $H_{applied}$ is applied magnetic field strength and *f* represents the frequency of the applied magnetic field.

Results and Discussion

XRD Analysis

Figure 1 shows the XRD patterns of LSMO MNPs with different components. All the XRD patterns correspond to the characteristic peaks of LSMO [11], except for the small peaks of La(OH)$_3$ in (b) and (c). The existence of unreacted La(OH)$_3$ is due to that the atomic size of La

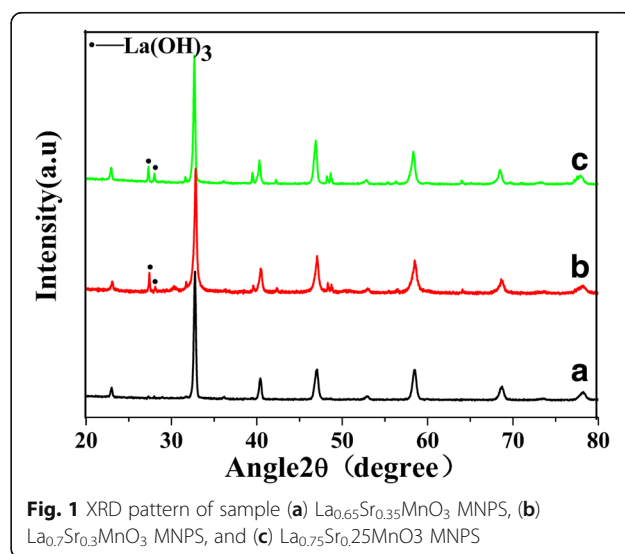**Fig. 1** XRD pattern of sample (**a**) La$_{0.65}$Sr$_{0.35}$MnO$_3$ MNPS, (**b**) La$_{0.7}$Sr$_{0.3}$MnO$_3$ MNPS, and (**c**) La$_{0.75}$Sr$_{0.25}$MnO3 MNPS

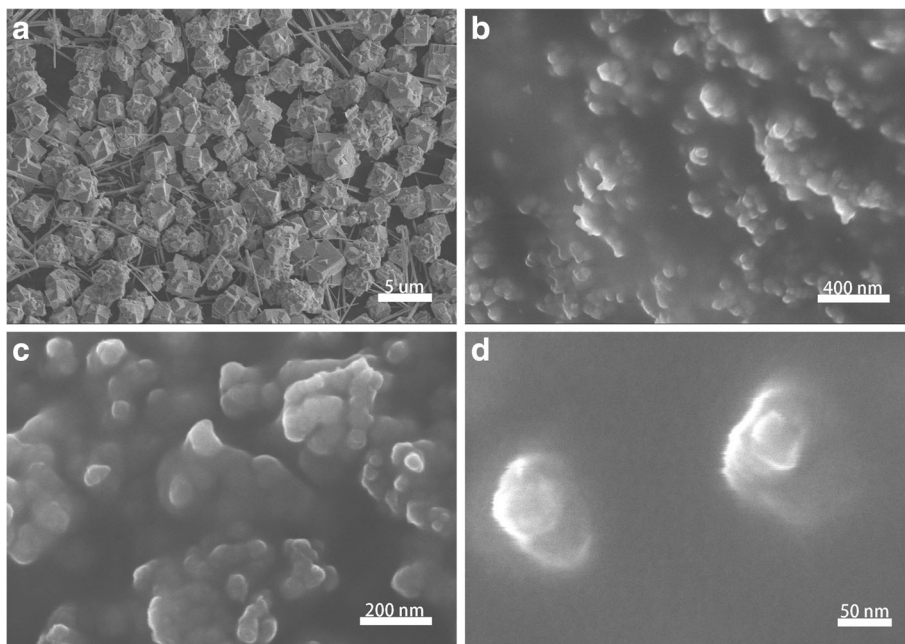Chen *et al. Nanoscale Research Letters* (2016) 11:538

Page 3 of 6

Fig. 2 a SEM image of the production of hydrothermal reaction. **b–d** SEM images of ball milled sample

is larger than that of Sr and is hard to enter the A site of the crystal structure of perovskite. As $La(OH)_3$ is non-magnetic and its amount is small, it has slim influence on the magnetic properties of the samples. The average grain size of LSMO MNPs calculated from Scherrer equation is about 30 nm for all samples.

SEM and TEM Analysis

The detailed surface morphologies of the samples were measured by SEM, and the corresponding images for all samples are presented in Fig. 2a–d, (Additional file 1). No Au sputtering was performed before the test of morphologies. From the image (a) it can be observed
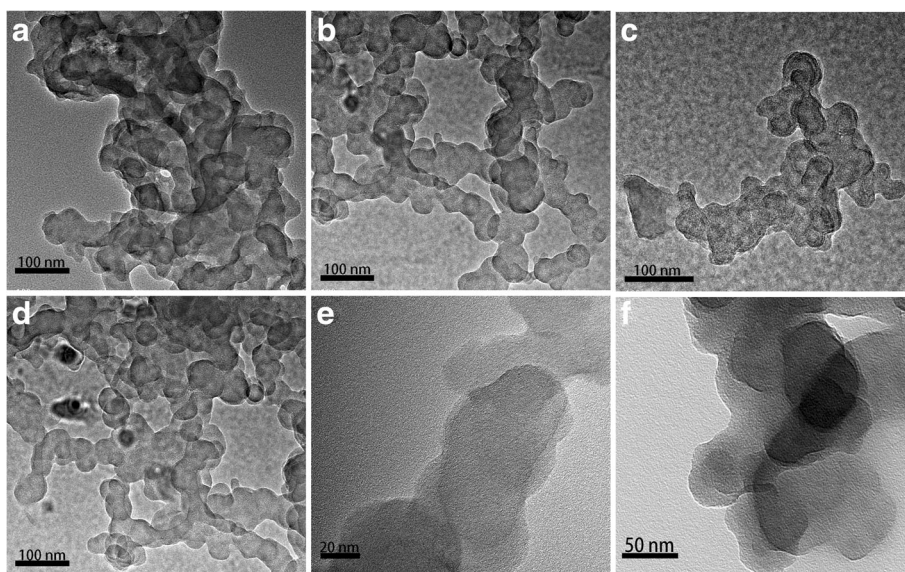

Fig. 3 a TEM image of HA-coated $La_{0.75}Sr_{0.25}MnO_3$ MNPs. **b** HA-coated $La_{0.7}Sr_{0.3}MnO_3$ MNPs. **c** HA-coated $La_{0.65}Sr_{0.35}MnO_3$ MNPs, and **d** OA-coated $La_{0.7}Sr_{0.3}MnO_3$ MNPs. **e–f** Brush-fire close-up of HA-coated $La_{0.7}Sr_{0.3}MnO_3$ nanoparticles

Chen *et al. Nanoscale Research Letters* (2016) 11:538
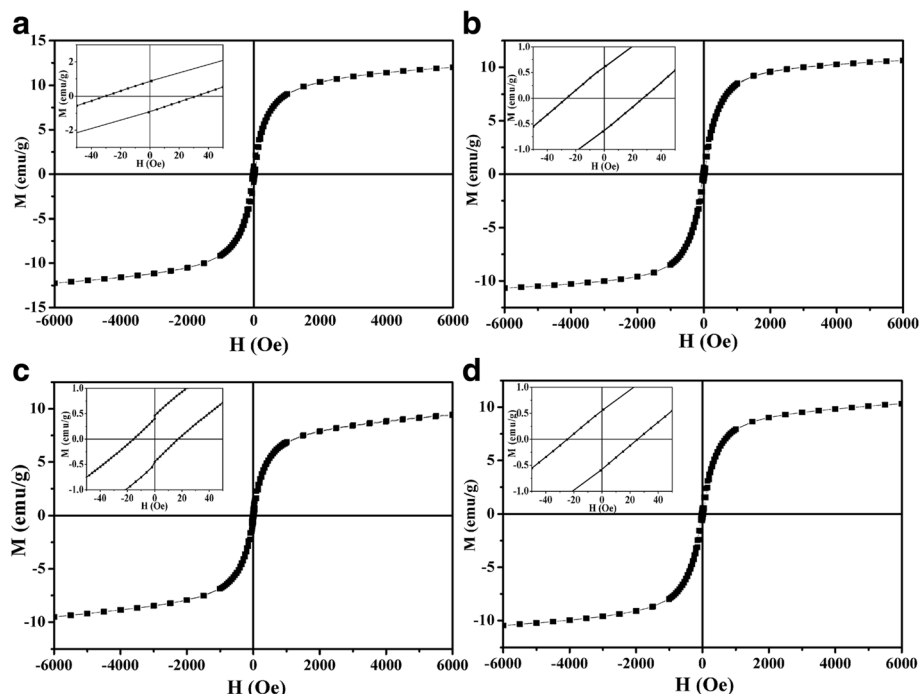
Page 4 of 6

Fig. 4 Hysteresis loops of S1(**a**), S2(**b**), S3(**c**), and S4(**d**) at 300 K

that the size of most grains before high-energy ball milling is in the micro level. The images b–d show that the particle size of the sample after high-energy ball milling with surfactant is ~100 nm. The TEM images of the samples were also measured (Fig. 3). It is obvious that the morphology of the particles is non-spherical and their connections are very loose. The nanoparticles size of LSMO coated by OA or HA is almost the same. In some previous studies on nanoparticles with specific sizes in the range of 5–

10 nm, the particles could be rapidly removed through hextravasation and renal clearance. On the other hand, the particles with size >200 nm could be sequestered by the spleen and eventually removed by the phagocytes. This could pose a detrimental risk of pulmonary embolism [20, 21], so the LSMO MNPs with size less than100 nm is a security dimension for hyperthermia application.

Magnetic Properties Measurement

Figure 4 shows the hysteresis loops of our samples at 300 K. The magnetization value (M_s) decreases with the increase of Sr concentration. Note that the magnetization for all samples does not reach saturation in the applied magnetic field up to 6000 Oe. The remanence (M_r) values are 0.85, 0.79, 0.54, and 0.52 emu g^{-1}, and the coercivity (H_c) values are 31.4, 23.6, 20, and 24.5 Oe for S1, S2, S3, and S4, respectively. The M_r and H_c values further confirm the size of MNPs is in nano level. The M versus T curves at a magnetic field of 5000 Oe were measured for all samples in order to confirm the T_c, the dM/dT versus T curve was calculated, and the position of the lowest value of dM/dT was recognized as average T_c of all MNPs. As Fig. 5 shows, the T_c of S1, S2, S3, S4 are 44 °C, 44.3 °C, 49.2 °C, and 43.9 °C, respectively. This result shows that S1, S2, and S4 are more suitable for magnetic hyperthermia.
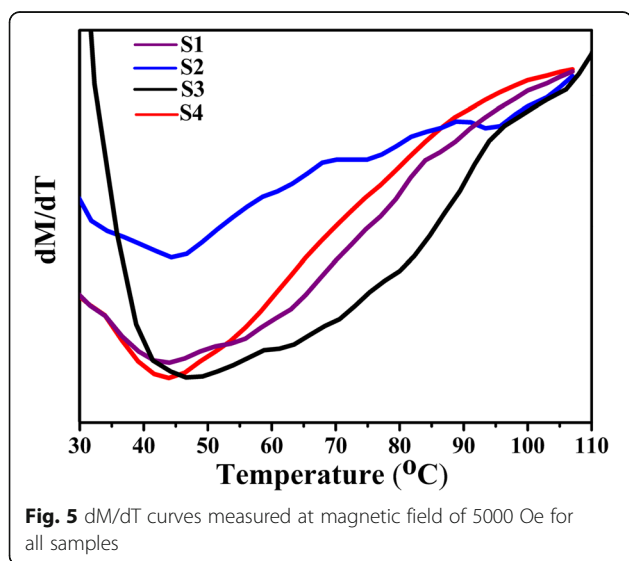

Fig. 5 dM/dT curves measured at magnetic field of 5000 Oe for all samples
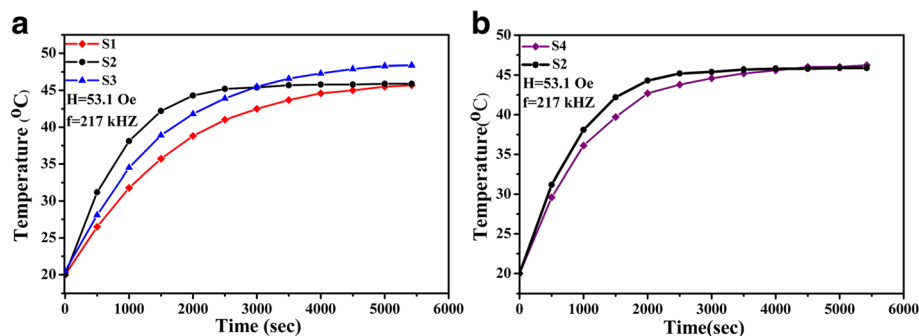
Chen *et al. Nanoscale Research Letters* (2016) 11:538

Page 5 of 6

Fig. 6 a Temperature versus time curve for HA-coated samples at AC magnetic fields. **b** Temperature versus time curve for HA-coated $La_{0.7}Sr_{0.3}MnO_3$ (S2) and OA-coated $La_{0.7}Sr_{0.3}MnO_3$ (S4) at AC magnetic field

Magnetic Heating Experiments

Figure 6 represents the temperature variation curves obtained after applying an alternating magnetic field on samples which were dispersed in water with a concentration of 6 mg/ml. All these heating curves show a monotonic rise in temperature with the increase in time. Figure 6a shows the curves of HA-coated samples at the field of $H = 53.1$ Oe and $f = 217$ kHz. It is observed that the saturation temperature of S1 and S2 is about 46 °C. That could satisfy the demand of temperature for mild hyperthermia treating [15, 17, 22]. Whereas, S3 keeps on heating until the temperature is up to 48 °C. That could be attributed to its higher T_c. Among the three samples of Fig. 6a, S2 possesses the best heating ability since its initial slope of the temperature rising line is the largest. Comparing to traditional OA-coated MNPs sample S4, the heating ability of S2 is also better, as shown Fig. 6b [12].

SAR and ESAR values of our samples are listed in Table 1. ESAR values of LSMO MNPs reported by other articles are also listed as a comparison. The larger SAR of S2 may be explained by its larger area within the hysteresis loop which is indicated by its higher remanence and similar coercivity to other samples' ones (Fig. 4). The ESAR value of S2 is obviously higher than other reported results, indicating a

better energy converting ability under alternating magnetic field. For the efficacy and safety of the hyperthermia treatment, the heat generated should be within the mild hyperthermia range of 41–46 °C and has good cell compatibility. In our experiment work, HA-coated $La_{0.7}Sr_{0.3}MnO_3$ magnetic fluid could meet these two demands.

Conclusions

$La_{1-x}Sr_xMnO_3$ ($0.25 \le \times \le 0.35$) MNPs were successfully synthesized and coated with HA as surfactant. The HA-coated $La_{0.7}Sr_{0.3}MnO_3$ magnetic fluid with the saturation heating temperature of 45.7 °C and magnetic particle size of ~100 nm could satisfy the requirements of the mild hyperthermia temperature range (41–46 °C) and good cell compatibility for therapeutic application. Moreover, the ESAR value of HA-coated $La_{0.7}Sr_{0.3}MnO_3$ magnetic fluid is much higher compared with the other reported experiment results. Combined with the targeting ability of HA to tumor, we deemed that the HA-coated $La_{0.7}Sr_{0.3}MnO_3$ magnetic fluid will be a good candidate for hyperthermia treatment. The improved particle dispersibility and ESAR are favorable to the future applications of coated MNPs in biomedical field.

Table 1 Heating efficiency of samples and references

Sample	H (kA/m)	$H \cdot f (Am^{-1}S^{-1})$	T_{max}(°C)	SAR(W/g)	ESAR(W/g $\cdot$ kHz $\cdot$ (kA/m)^2)
S1	4.23	9.17×10^8	45.5	10.3 ± 0.1	$(2.67 \pm 0.04) \times 10^{-3}$
S2	4.23	9.17×10^8	45.7	18.2 ± 0.2	$(5.73 \pm 0.08) \times 10^{-3}$
S3	4.23	9.17×10^8	48.4	14.5 ± 0.2	$(3.66 \pm 0.06) \times 10^{-3}$
S4	4.23	9.17×10^8	46.1	16.1 ± 0.2	$(4.21 \pm 0.06) \times 10^{-3}$
Ref.[22]	10.95	1.92×10^9	46.7	56	2.7×10^{-3}
Ref.[12]	26.7	7.12×10^9	56	40.22	2.11×10^{-4}

Chen *et al. Nanoscale Research Letters* (2016) 11:538

Page 6 of 6

Additional file

Abbreviation
ESAR: Effective specific absorption rate; HA: Hyaluronic acid; MNPs: Magnetic nanoparticles; OA: Oleic acid; SAR: Specific absorption rate; SEM: Scanning electron microscopy; TEM: Transmission electron microscopy

Authors' Contributions
TW, YW, ML, XL, and JWC conceived and coordinated the project. YWC and YW carried out the experimental work. YWC wrote the manuscript. All authors read and approved the manuscript.

Competing Interests
The authors declare that they have no competing interests.

Author details
[1]Key Laboratory for Magnetism and Magnetic Materials of the Ministry of Education, Lanzhou University, Lanzhou 730000, China. [2]Key Laboratory of Opto-Electronic Technology and Intelligent Control, Ministry of Education, Lanzhou Jiaotong University, Lanzhou 730070, China.

References
1. Zhang X, Fan J, Xu L, Hu D, Zhang W, Zhu Y (2016) Magnetic and magnetocaloric properties of nanocrystalline $La_{0.5}Sr_{0.5}MnO_3$. Ceram Int 42: 1476–1481.
2. Huang Y-H, Yan C-H, Wang S, Luo F, Wang Z-M, Liao C-S, Xu G-X (2001) Chemical synthesis of $La_{0.7}Sr_{0.3}MnO_3$/silica homogeneous nanocomposites. J Mater Chem 11:3296–3299
3. Kumar CS, Mohammad F (2011) Magnetic nanomaterials for hyperthermia-based therapy and controlled drug delivery. Adv Drug Deliv Rev 63:789–808.
4. Strobl FF, Azam H, Schwarz JB, Paprottka PM, Geith T, Abdel-Rahman S, Zilles B, Lindner LH, Reiser MF, Trumm CG (2016) CT fluoroscopy-guided closed-tip catheter placement before regional hyperthermia treatment of soft tissue sarcomas: 5-Year experience in 35 consecutive patients. Int J Hyperthermia 32:151–158.
5. Myerson RJ, Moros EG, Diederich CJ, Haemmerich D, Hurwitz MD, Hsu ICJ, McGough RJ, Nau WH, Straube WL, Turner PF, Vujaskovic Z, Stauffer PR (2014) Components of a hyperthermia clinic: Recommendations for staffing, equipment, and treatment monitoring. Int J Hyperthermia 30:1–5.
6. Mendo SG, Alves AF, Ferreira LP, Cruz MM, Mendonça MH, Godinho M, Carvalho MD, New J (2015) Hyperthermia studies of ferrite nanoparticles synthesized in the presence of cotton. Chem 39:7182–7193.
7. Haw C, Chiu W, Abdul Rahman S, Khiew P, Radiman S, Abdul Shukor R, Hamid MAA, Ghazali N (2016) The design of new magnetic-photocatalyst nanocomposites ($CoFe_2O_4$–TiO_2) as smart nanomaterials for recyclable-photocatalysis applications. New J Chem 40:1124–1136.
8. Jadhav SV, Nikam DS, Mali SS, Hong CK, Pawar SH (2014) The influence of coating on the structural, magnetic and colloidal properties of LSMO manganite and the heating mechanism for magnetic fluid hyperthermia application. New Journal of Chemistry 38:3678.
9. Kulkarni VM, Bodas D, Paknikar KM (2015) Lanthanum strontium manganese oxide (LSMO) nanoparticles: a versatile platform for anticancer therapy. RSC Adv 5:60254–60263.
10. Thorat ND, Shinde KP, Pawar SH, Barick KC, Betty CA, Ningthoujam RS (2012) Polyvinyl alcohol: an efficient fuel for synthesis of superparamagnetic LSMO nanoparticles for biomedical application. Dalton Trans 41:3060–3071.
11. Makovec D, Goršak T, Zupan K, Lisjak D (2013) Hydrothermal synthesis of $La_{1-x}Sr_xMnO_3$ dendrites. J Cryst Growth 375:78–83.
12. Thorat ND, Khot VM, Salunkhe AB, Prasad AI, Ningthoujam RS, Pawar SH (2013) Surface functionalized LSMO nanoparticles with improved colloidal stability for hyperthermia applications. J Phys D Appl Phys 46:105003.
13. Zhu H, Yang D, Zhu L, Yang H, Jin D, Yao K (2007) A facile two-step hydrothermal route for the synthesis of γ-Fe_2O_3 nanocrystals and their magnetic properties. J Mater Sci 42:9205–9209.
14. Wang S, Huang K, Zheng B, Zhang J, Feng S (2013) Mild hydrothermal synthesis and physical property of perovskite Sr doped $LaCrO_3$. Mater Lett 101:86–89.
15. Thorat ND, Khot VM, Salunkhe AB, Ningthoujam RS, Pawar SH (2013) Functionalization of La(0.7)Sr(0.3)MnO3 nanoparticles with polymer: studies on enhanced hyperthermia and biocompatibility properties for biomedical applications. Colloids Surf B Biointerfaces 104:40–47.
16. Ferguson RM, Khandhar AP, Jonasson C, Blomgren J, Johansson C, Krishnan KM (2013) Size-Dependent Relaxation Properties of Monodisperse Magnetite Nanoparticles Measured Over Seven Decades of Frequency by AC Susceptometry. IEEE Trans Magn 49:3441–3444.
17. Thorat ND, Otari SV, Patil RM, Khot VM, Prasad AI, Ningthoujam RS, Pawar SH (2013) Enhanced colloidal stability of polymer coated $La_{0.7}Sr_{0.3}MnO_3$ nanoparticles in physiological media for hyperthermia application. Colloids Surf B Biointerfaces 111:264–269.
18. Deatsch AE, Evans BA (2014) Heating efficiency in magnetic nanoparticle hyperthermia. J Magn Magn Mater 354:163–172.
19. Manh DH, Phong PT, Nam PH, Tung DK, Phuc NX, Lee I-J, Physica B (2014) Structural and magnetic study of $La_{0.7}Sr_{0.3}MnO_3$ nanoparticles and AC magnetic heating characteristics for hyperthermia applications. Condensed Matter 444:94–102.
20. Choi HS, Liu W, Misra P, Tanaka E, Zimmer JP, Itty Ipe B, Bawendi MG, Frangioni JV (2007) Renal clearance of quantum dots. Nat Biotechnol 25: 1165–1170.
21. Zhou Y, Zhu X, Li S (2015) Effect of particle size on magnetic and electric transport properties of La(0.67)Sr(0.33)MnO3 coatings. Phys Chem Chem Phys 17:31161–31169.
22. McBride K, Cook J, Gray S, Felton S, Stella L, Poulidi D (2016) Evaluation of $La_{1-x}Sr_xMnO_3$(0 ≤ x < 0.4) synthesised via a modified sol–gel method as mediators for magnetic fluid hyperthermia. CrstEngComm 18:407–416